Antennas in Automobile Radar

Abstract

Automobile radars are under investigation since the 1960s. The first operational systems are on the market since 1992 for buses and trucks and 1999 for passenger cars, both in the frequency range around 24 as well as 76.5 GHz; a new frequency band for medium- and short-range sensors from 77 to 81 GHz has been allocated recently in Europe. Requirements for the sensor antennas are high gain and low loss combined with small size and depth for vehicle integration. Great challenges are due to the millimeter-wave frequency range, and a great cost pressure for this commercial application determines design and fabrication. Consequently, planar antennas are dominating in the lower frequency range, while lens and reflector antennas had been the first choice at 76.5 GHz, partly in folded configurations. With increasing requirements toward a much more detailed view on the scenery in front or around the vehicle, multi-beam antennas or scanning antennas have been designed. For actual systems, digital beamforming with a number of integrated antennas is in use or under development, and also MIMO concepts will be exploited. With such development, antennas for automotive radar no longer can be considered as stand-alone devices, but will be part of an "imaging" system including multiple transmit/receive units and digital signal processing.
General antenna concepts, partly including system aspects, as well as several realized antenna and sensor configurations will be described in detail in this chapter.
Keywords Automotive radar - Millimeter-wave radar - Radar antennas - Microstrip antenna - Grid antenna - Reflector antennas - Lens antennas - Slotted waveguide array - Dielectric antenna

Introduction

With increasing traffic density, an increasing interest has emerged for additional electronic vision to improve comfort and safety, including video cameras, infrared sensors, laser, or radar. Although radar does not provide optical resolution, it has the great advantage of being mostly insensitive to fog or rain, it works independently on ambient light, and it directly provides speed based on the Doppler effect. Consequently, radar was considered as automotive sensor already back to 1959, when Cadillac presented two radar sensors in its experimental car "Cadillac Cyclone" (Cadillac 2013). No detailed information has been published, but the ogive-shaped radomes indicate military-type radars. In the 1970s, a number of companies again investigated automotive radars, starting at 10, 16, and later on 35 GHz (Meinel and Dickmann 2013) (Fig. 1). Later on, other systems were considered at 60 GHz (mostly in Japan, using the license-free ISM band) or 94 GHz based on military developments. The first commercial radar for collision avoidance was introduced in 1992 in the USA by VORAD for buses and trucks, working at 24 GHz (Woll 1995) (Fig. 2). It helped in reducing crashes, but was not really accepted by the drivers who felt too much controlled by this system. In 1998/1999, the first commercial radar in a passenger car was introduced by Mercedes in Germany, working in the 76-77 GHz frequency band, followed by other car manufacturers. These first radar sensors were used mostly in comfort functions, supporting an automatic speed control by keeping a safe distance to the preceding vehicle (adaptive cruise control, ACC).

Fig. 1
Vehicle with a first 35 GHz radar (separate parabolic reflector antennas for transmit and receive, photograph TELEFUNKEN)

Fig. 2
VORAD radar in front of a bus (own photograph)

The aim for further developments during the last years has been to make radar available for safety functions like forward collision alert, rear traffic crossing alert, blind spot detection, or side-impact warning; the latest developments include emergency breaking and autonomous stop-and-go driving (Mercedes E- and S-class). According to such different functions, sensors have to look into all directions around the vehicle with differently defined scanning and distance relations. Rear traffic crossing alert and blind spot detection, for example, operate in the near range and simply give information whether one or more targets are present in a certain area, whereas ACC and forward collision alert have to scan the entire traffic scene not only in the near range but also - dependent on the maximum speed of the object - in the mid- and far range. Typical range designations are low-range (LRR, up to a few 10 m), medium-range (MRR, about 40-100 m), and long-range (LRR, up to 200 m or even 250 m) radars. As a consequence, a much more flexible and wider field of view is required compared to the first applications, resulting in some kind of "imaging" of the scenery in front of the sensor. This, of course, has to be mapped to the antenna concepts, partly in combination with modified overall sensor arrangements, including multi-beam antennas, scanning antennas, switched antenna concepts, and beamforming approaches with multiple transmit and receive antennas. Recent trends show a change from the scanning or multi-beam antenna principle to the digital beamforming with increasing functional transfer to digital signal processing. As a consequence, automotive antenna concepts must not be considered independently from the overall system concept, but increasingly, the overall range and way of "viewing" the interesting range of angles is determined by an optimal combination of antenna elements, RF front end, and signal processing. The actual field of view of the sensor therefore is determined by the antenna or antenna system diagram but also by the required angle-dependent range (with possibly

lower gain in directions away from the main lobe), the minimum radar cross section, and the required minimum signal-to-noise ratio.

Furthermore, when designing automotive systems including antennas, the engineer faces the task that all components must be suitable for mass production, operate in a temperature range from −40 °C to 85 °C or even 105 °C, and be shockproof, and the entire arrangement has to be compact in size. The implications of all these on the choice of materials and even the performance should not be underestimated.

Present frequencies allocations for short range are in the 24.05-24.25 GHz frequency range (ISM band), a 4 GHz wide band around 24 GHz, but with different allocations and restrictions in different countries, and the 76-77 GHz range for the far range. Recently, in the EU the band from 77 to 81 GHz has been allocated for short range and mid-range; efforts are undertaken to make this frequency range available for automotive radar worldwide. In the near future, almost all long- or mid-range antennas will operate in the 76-81 GHz range.

Key Properties of Automotive Radar

Automotive radar sensors provide information about other vehicles, pedestrians, and the road environment by measurement of the flight time of the electromagnetic wave from the radar to a target and back; relative speed is determined, extracting the Doppler frequency shift, and angular information is given by the antenna characteristics. Automotive sensors typically use either a pulse modulation (Gresham et al. 2004) or frequency-modulated constant wave (FMCW) signals with sawtooth or triangular frequency modulation (Hymans and Lait 1960). Most of the automotive pulse sensors operate in a sampling mode with some similarity to a sampling oscilloscope (Fig. 3). The received pulses are down converted with a pulse delayed by a time τ; an intermediate-frequency (IF) signal occurs only if the time of flight of the pulse is identical to the delay. Together with a low-pass filter (LPF) for the IF signal, bandwidth at the receiver output can be considerably reduced, and a further digital processing with moderate speed is possible. For the FMCW sensor, a signal with a linear frequency ramp is transmitted and then received with the respective delay time (Fig. 4). Down conversion with the actual transmitter signal then results in an IF signal, the frequency of which is proportional to the target distance. A typical further processing is done via analog-digital converter (ADC) and fast Fourier transform (FFT). As transmit/receive diplexer, mostly 3 dB couplers are used to avoid complicated and expensive circulators (as indicated in Fig. 3), or even individual antenna elements are used for transmitting and receiving (as indicated in Fig. 4).

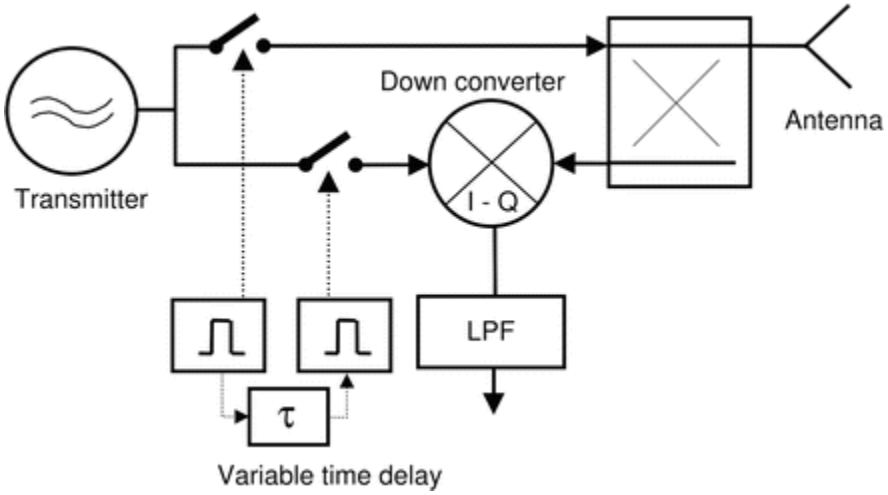

Fig. 3
Basic block diagram of an automotive pulse radar

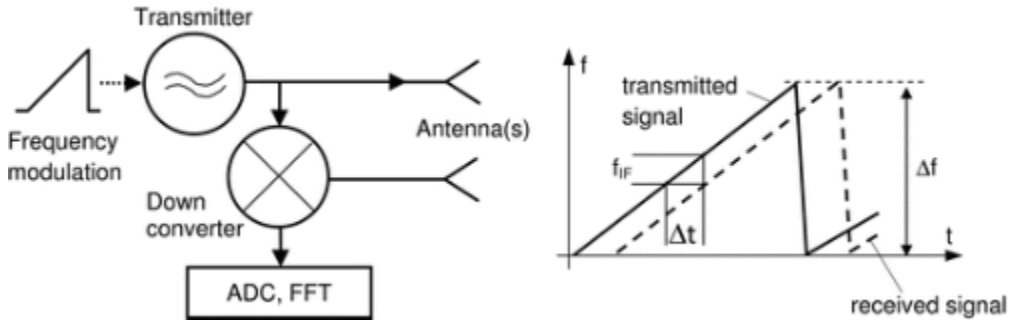

Fig. 4
Basic block diagram and time-frequency diagram of an FMCW radar

In general, signal bandwidth, either via pulse width or FMCW frequency deviation, determines the minimum range resolution ΔR (separation between two targets):

$$\Delta R = c_0/(2\Delta f) \quad (1)$$

with c_0 as speed of light and Δf the modulation bandwidth. Typical values of ΔR range from about 1 m for early systems to some cm for newer short-range broadband systems (up to some GHz of bandwidth).
While for the first radar sensors, the RF circuits of the front ends were built based on discrete devices like Gunn elements and Schottky diodes, monolithic microwave integrated circuits (MMIC) based on GaAs (Camiade et al. 2000) and silicon-germanium (SiGe) are available today. SiGe MMICs even provide several RF front ends and some basic digital circuits on a single chip (Winkler et al. 2008).
The angular or cross-range observation depends on the sensor application and is determined by its antenna arrangement. In an early stage, when automotive sensors were used solely in comfort functions supporting the automatic speed control by keeping a safe distance to the preceding vehicle, a few (switched) narrow antenna beams were sufficient to monitor the own and adjacent lanes on a highway. Today, for safety purposes both for highway and for dense urban traffic scenarios, much more sophisticated antenna and overall system concepts are required.

Types of Antennas for Automotive Radar

General Requirements and Properties of Automotive Antennas

In general, the beamwidth of antennas is related directly to the physical size of an antenna. A rule of thumb estimates the 3 dB beamwidth ΔΦ by

$$\Delta\Phi = 60^\circ \ \lambda/D \quad (2)$$

where λ is the free space wavelength and D the overall antenna dimension in the respective plane. Requirements for a long-range sensor to restrict the 3 dB beamwidth to a 3.5 m-wide highway lane at a distance of about 50 m result in a beamwidth of 4° in azimuth and an antenna width of 15 wavelengths. This immediately shows that millimeter-wave frequencies are required to be able to integrate a radar sensor into the front of a car. At 77 GHz, this results in an antenna width of 60-80 mm. In elevation, a radar sensor should avoid strongly illuminating any bridge or traffic signs above the street (typically in a height of at least 5 m); this results in similar beamwidth requirements. Antenna gain then is in the range of 30 dB. To also observe neighboring lanes or operating in curves, several beams or some moderate beam scanning is required. At 24 GHz, antenna size and beamwidth typically are larger. Mid- and near-range systems have wider beamwidths and lower gain but require a wider angle of view by scanning, multiple beams, or beamforming.
Antenna losses should be low to maintain transmit gain as high as possible and not to deteriorate the receiver noise figure too much. Sidelobe levels need to be low enough to avoid false detection of targets at larger angles.
Compared to typical targets, wavelengths of about 12 and 4 mm at 24 and 77 GHz, respectively, are generally small, so polarization does hardly have any influence on target reflections. Some additional information may be gained if also

orthogonal polarization was received, but this would add the implications of dual-polarization antennas and doubling the receiver part of the radar. In some sensors, polarization is adjusted at 45°; in this case, direct radiation from a radar into that of an oncoming vehicle is reduced. Ground reflections, however, will mostly foil the effects of this measure.
The antenna depth is of concern in integrating the sensor into the vehicle. Finally, antenna fabrication and integration into the sensor should be easy, reproducible, and cost-effective. The overall sensor including the antenna has to withstand shock, vibration, and the required automotive temperature range as mentioned above.

Reflector and Lens Antennas

In first test as well as in the first series versions of automotive radars, standard types of antennas were used, including horn antennas and parabolic reflectors. For sensors used in a car, antenna depth is of great concern for integration into the vehicle surface as well. A prominent example is a lens antenna with short focal length (Binzer et al. 2007), included in the commercial LRR3 sensor by Bosch. Another way to reduce the antenna depth is by "folding" the ray path of reflector or lens antennas as presented in Fig. 5 (Gresham et al. 2001; Millitech 1994). In these antennas, a feed initially radiates against a polarizing filter, and the wave is reflected back toward a planar structure where the wave is reflected again, but with a polarization twisted by 90°.

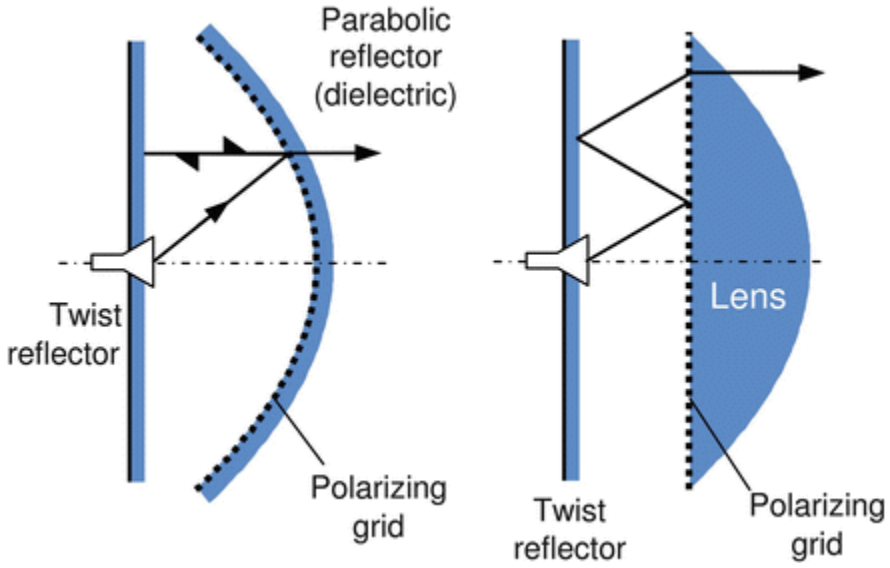

Fig. 5
Folded reflector (left) and lens antennas (right)

Such polarization twisting can be achieved by structures as shown in Fig. 6. The incident wave is polarized at 45° with respect to the axes of the reflecting structure (grid or rectangular patches). For the analysis of the reflected wave, the field is decomposed into components parallel to the two axes. In the case of the grid, the component parallel to the grid wires is reflected directly, while the orthogonal component passes the grid and is reflected at the ground plane placed a quarter of a wavelength behind the grid, resulting in an overall detour of half a wavelength or 180°. Combining the outgoing two components again, a wave results with a polarization twisted by 90°. For the structure with rectangular patches, the dimensions of the patches are selected in such a way that the reflection phase angles for the two components parallel to the patch axes differ by 180°, resulting in the same 90° twisting of the polarization. In this case, the thickness of the substrate does not need to be a quarter wavelength thick.

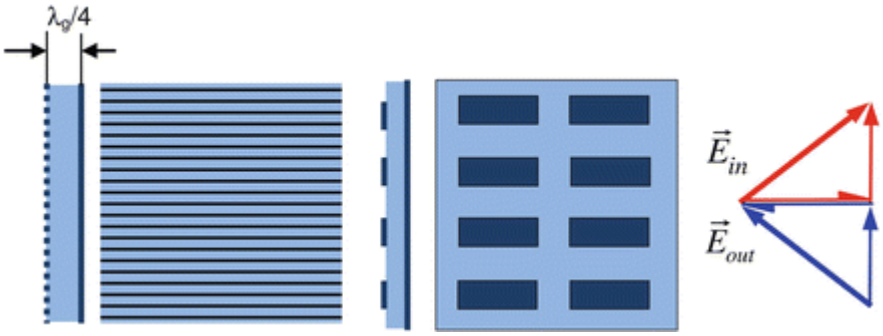

Fig. 6
Principles for polarization twisting (λ_g, wavelength in the dielectric)

In Menzel et al. (2002), the complex lens or curved reflector has been replaced by a planar printed structure (reflectarray) which, at the same time, can perform focusing of an incident spherical wave and twist the polarization (Fig. 7, top). The wave from a feed horn is incident on the polarizing grid (with its polarization parallel to the grid lines) and is reflected back to the planar array. Typical reflecting elements of such a reflectarray are rectangular patches which are oriented at an angle of 45° with respect to the incident polarization. Ninety degree twisting of the wave polarization is achieved in the same way as described above. Furthermore, combinations of the length and width of the patches can be selected to additionally give the required absolute phase shift to form an outgoing plane wave. Such an antenna with three beams (generated by three different feed locations) has been implemented into the second generation of Mercedes radars (Fig. 7, bottom), and this principle is also included in the third-generation sensor ARS 300 delivered by Continental (see the second application example in this chapter).

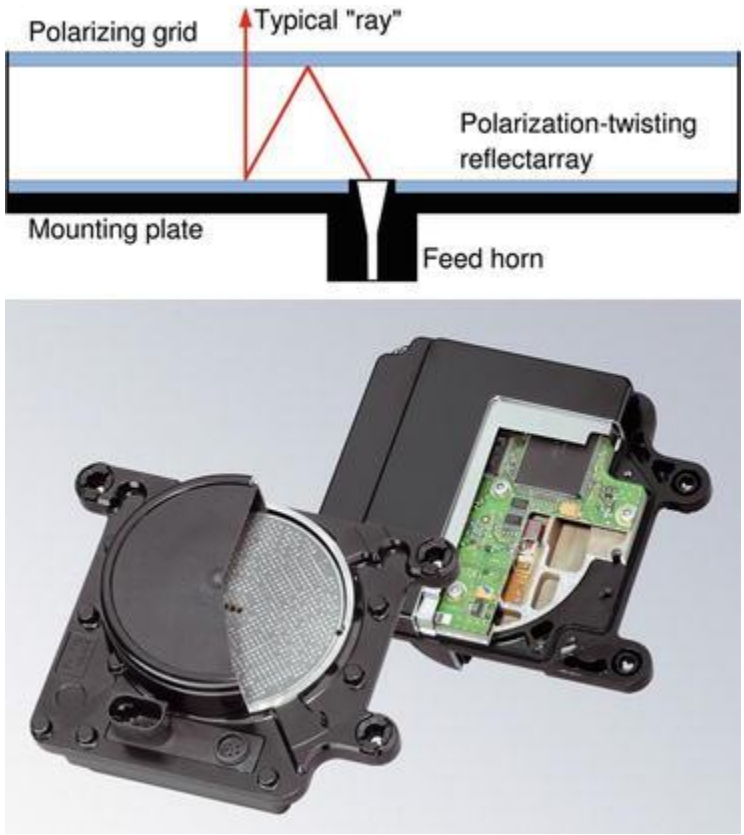

Fig. 7
Cross section and photograph (press photograph Continental ADC) of a folded reflectarray antenna (frequency 76.5 GHz, antenna diameter 90 mm, depth 23 mm)

In general, lens and reflector antennas exhibit very low loss, advantageous in combination with millimeter-wave

semiconductor elements for power generation of quite moderate level, but they require a non-negligible depth of a few cm; thus, purely planar antennas are gaining more and more interest.

Planar Antennas

Planar antennas are found in various forms; the most common types are microstrip antennas (Carver and Mink 1981; James et al. 1981); for details see also the respective chapter in this book. Most often, half-wavelength resonators or dipoles (patch antennas) or open ends of microstrip stubs (Fig. 8) are employed as single antenna elements. Figure 8b depicts the longitudinal cross section of a radiating patch including the principal electric field distribution. In a very simplified model, the stray fields at the ends are the radiating sources - with this half-wavelength patch, the horizontal components of the stray field have the same direction and combine in phase for a broadside radiation (the respective stray fields at the patch sides are in antiphase and cancel to a great extent). For narrower beams and higher gain, such elements can be combined in series and/or parallel arrangements (Fig. 8c, d) to form antenna arrays with the required overall antenna diagram. In Fig. 8c and d, the red arrows show the horizontal stray fields at the radiating edges and indicate the in-phase behavior, resulting in a broadside radiation.

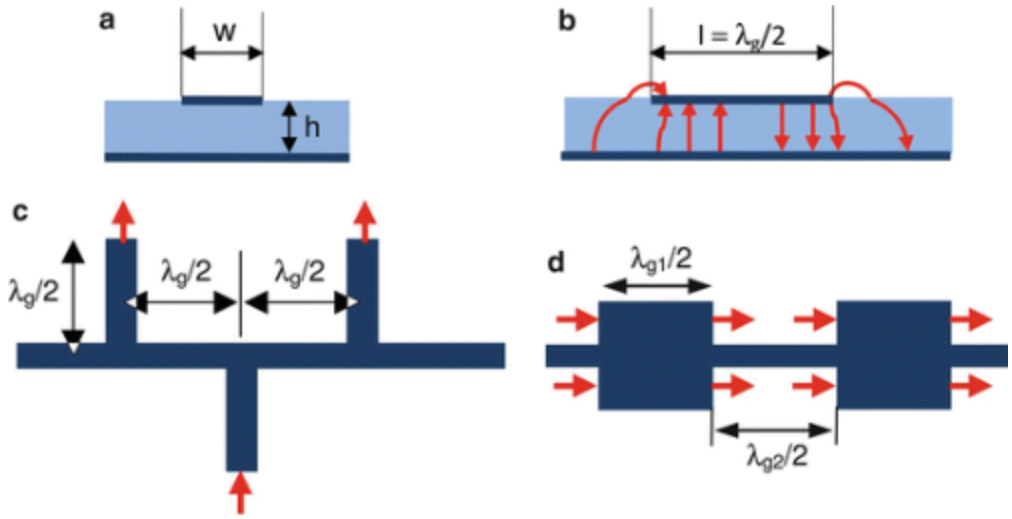

Fig. 8
Microstrip antennas : (a) microstrip cross section, (b) longitudinal cross section with an electric field of a half-wavelength resonator (patch antenna), (c) chain of radiating open-ended microstrip stubs, (d) chain of microstrip patches connected by half-wavelength lines

Microstrip patches are resonators and typically exhibit bandwidths in the range of only a few percent with limited antenna efficiency, improving with lower dielectric constant of the substrate and increasing substrate thickness. The latter, however, leads to a higher degree of radiation by the feeding network as well as to the excitation of surface waves. Feed radiation may be mitigated by feeding the patch from the backside via a slot in the ground plane, but surface waves are more difficult to handle.

Single-patch antennas can be employed as feeding elements for a lens antenna (Binzer et al. (2007); see the first application example in this chapter); arrays of microstrip patches can be used directly as automotive antennas (Gresham et al. 2004; Winkler et al. 2008; Russell et al. 1997; Tokoro et al. 2003). With increasing geometrical dimensions of patch antenna arrays, feed network losses, especially for arrays with corporate feed networks, may pose a severe limit for antenna size. Series feeding of patches or open-ended stubs (Fig. 8) is based on connecting line segments of fixed length to ensure proper phase angle adjustment of each element; this however is valid only at a single frequency. Varying frequency, a progressive phase variation occurs from element to element, resulting in some degree of beam scan. For small array with relatively large beamwidth, this generally is of minor importance, but with an increasing length of a series-fed chain, beam scanning is no longer negligible.

Being predominantly resonating structures, patch antennas and radiating stubs exhibit limited bandwidth and increased losses; these effects pose a severe limitation for microstrip substrates with increased dielectric constant, e.g., for highly integrated circuits on low (or high)-temperature cofired ceramic (LTCC, HTCC) substrates. Already in the 1960s, a type of wire antenna was proposed, called grid antenna (Kraus 1964). Conti et al. (1981) proposed a microstrip version of such a

grid array antenna. This array consists of a double meander microstrip structure as depicted in Fig. 9, top. All segments are about half a guided wavelength long; the currents (plotted white in Fig. 9) in the longitudinal segments have the same direction and contribute in phase to radiation. As there are no strong resonances, this type of antenna is more broadband, even for high-dielectric -constant substrates, and less sensitive to tolerances. Several segments can be aligned together in series, and even two or more chain can be combined in parallel (Fig. 9, bottom). Feeding can be done at one end or at suitable positions within the chain by coaxial or probe-type feeds from the substrate backside (Bauer and Menzel 2011, Bauer et al. 2013), via slot coupling through the ground plane, or even with a symmetric stripline from the side (opening one of the loops of the antenna (Frei et al. 2011)). Feeding a grid antenna chain from one end results in an antenna with slight scanning properties; feeding it in the center results in two shorter sections with reduced scanning into opposite directions and thus in a more broadband design.

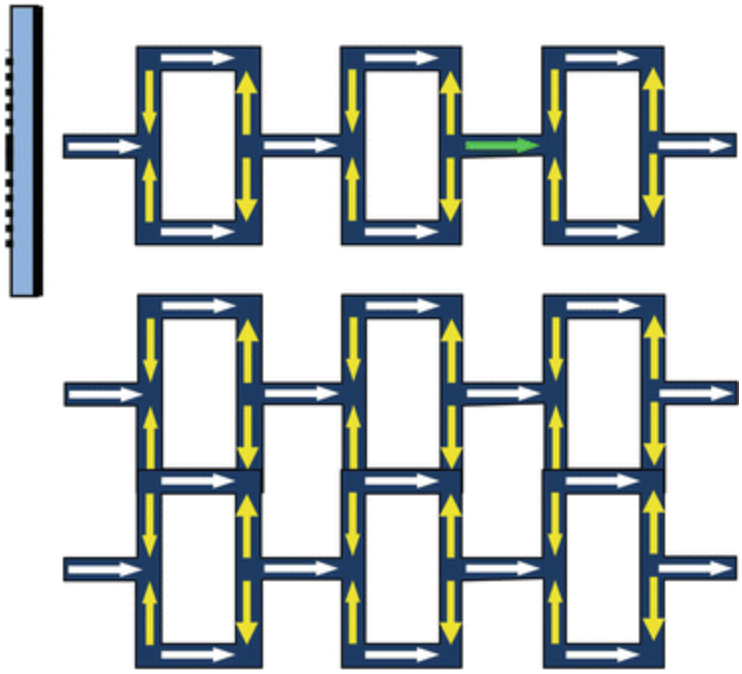

Fig. 9
Single- and double-row grid antenna

The grid antenna has been implemented in different types of application, e.g., 60 GHz communication (Zhang and Zhang 2012), or in an experimental LTCC front end for a short-range automotive sensor (Bauer et al. 2013); this will be described in more detail later on in this chapter.

A well-known type of antenna is the waveguide slotted array (Fig. 10). It consists of a metal waveguide with longitudinal or transversal slots. Once again, radiation from a number of slots superimpose in phase to form the desired radiation pattern. One approach to make this antenna suitable for automotive radar is to machine a waveguide pattern into a metal plate and to glue a metal foil with the slots on top of this (Sakakibara et al. 2006). For an easy and low-cost fabrication, however, a synthetic or substrate integrated waveguide (SIW) can be realized within a dielectric substrate where the sidewalls are formed by rows of vias (Hirokawa and Ando 2000; Xu et al. 2009; Massen et al. 2013). Slotted arrays based on SIW can even be realized with LTCC substrates. As waveguide width is reduced due to the dielectric filling of this waveguide, only longitudinal slots are used. A critical item is tolerances for the dimensions of the slots due to the high frequency and the (high) dielectric constant; with a novel shape of the slots including bends, this problem can be overcome to some extent (Bauer and Menzel 2013a). In some applications, a resonant cavity is placed above each slot, either by an additional metal plate including the cavities (Sakakibara et al. 2006) or integrated within a (LTCC) multilayer substrate (Shino et al. 2005; Bauer and Menzel 2013b), giving a more broadband and better radiation performance.

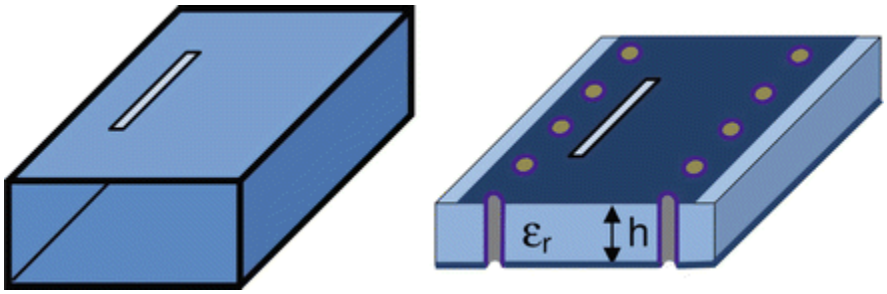

Fig. 10
Metal waveguide and substrate integrated waveguide (SIW) with radiating slots

As an example, an SIW slotted array is shown in Fig. 11, realized on a Rogers RO3003 substrate. It consists of three rows of SIW with 15 radiating slots in each row, together with a 1:3 power divider in the same technique. The longitudinal distance between the slots is half a wavelength with the SIW; the power distribution along the rows is controlled by the slot widths. An amplitude taper both within the rows and between the rows (unequal power divider) is selected to achieve a −20 dB sidelobe level. Details of the design procedure are given in Massen et al. (2013). H-plane radiation diagrams (perpendicular to the slots) at 78, 79, and 80 GHz are plotted in Fig. 12, together with the E-plane diagram at 79 GHz (the E-plane diagram does not change in the frequency range of interest). Beamwidths of 11° and 34° in H- and E-plane can be found. In both planes, the required sidelobe level is nearly met. A slight beam scan can be observed in the H-plane due to the series-fed slots. This array is one of six subarrays finally integrated on one substrate to form an antenna for digital beamforming (Massen et al. 2013).

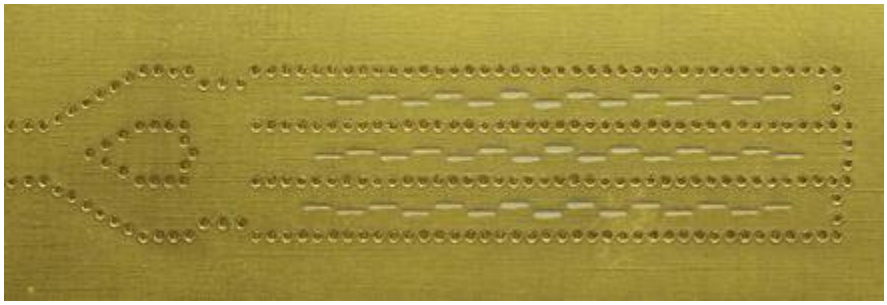

Fig. 11
Photograph of an SIW slotted array example (Massen et al. 2013, own photograph)

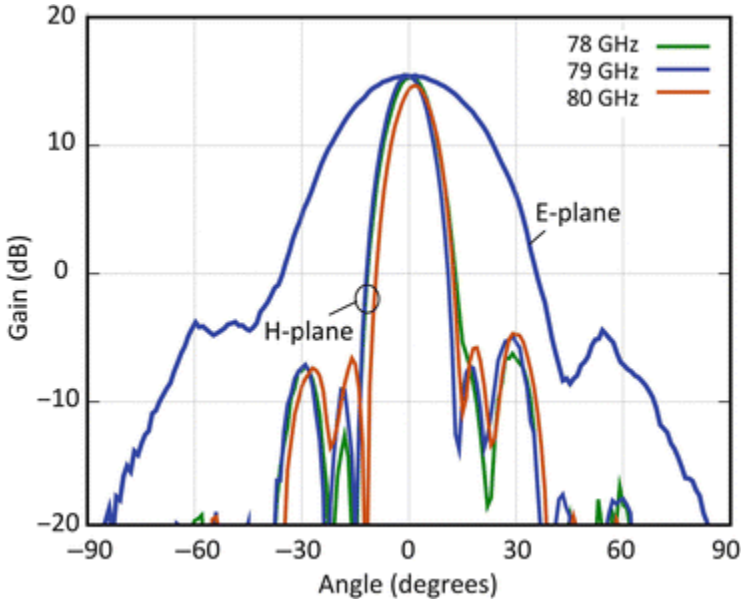

Fig. 12
Measured E- and H-plane radiation diagrams of the array shown in Fig.11

Digital Beamforming

Antenna elements of arrays or subarrays as described in the previous subsection often are connected by transmission lines to (larger) arrays and provide fixed beams. Antenna elements or subarrays can alternatively be connected to phase shifters (and attenuators), allowing electronic beam scanning (Fig. 13, left side); this typically results in relatively complex, lossy, and costly arrangements at mm-wave frequencies. An alternative approach is to use several antenna elements or subarrays and either switch these successively to a receiver or transmitter or connect them to multiple transmit/receive circuits, easily done with modern MMICs like in Winkler et al. (2008). Figure 13, right side, shows the example block diagram of a receiver with digital beamforming. The scene of interest is illuminated by a separate transmit antenna, or a combined transmit/receive circuit may be connected to one or (successively) several of the antenna elements. The receiver channels down convert and amplify the respective signals. The IF signals are sampled and converted to a sequence of digital values which can be processed further. After range processing for each channel, typically using an FFT for FMCW sensors, amplitude and phase angle are available for each range cell and receive channel. Multiplication with a complex number is equivalent to modify the amplitude and phase angle for the analog signal. A more efficient approach is based on the relations indicated in Fig. 14. An incident plane wave from a given slant angle is received by n receivers; according to the different path lengths, the signal at each receiver suffers a progressive delay (phase angle), resulting, after down conversion, in signals proportional to $\cos(i\, k_0\, d\, \sin\vartheta)$ with i, the number of the element; d, the distance between the elements; and k_0, the free space propagation constant. Accordingly, the spatial frequency of the sampled values indicated by the dotted line in Fig. 14 increases with increasing angle ϑ of incidence. As a consequence, applying another Fourier transform in cross range, different directions of wave incidence can be detected simultaneously, thus being able to measure the scenery in front of a car with high precision (Gresham et al. 2004; Asano et al. 2001; Stelzer et al. 2010). In comparison to analog beamforming with a phased array, this approach is referred to as digital beamforming.

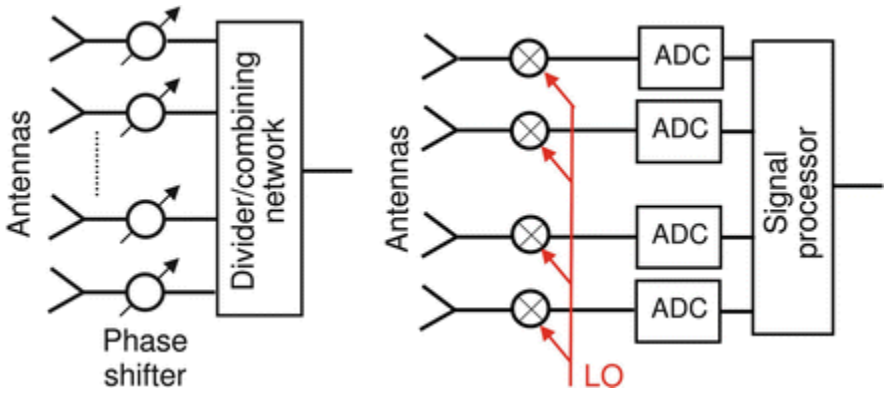

Fig. 13
Basic structures of phased array (left) and beamforming antenna (right)

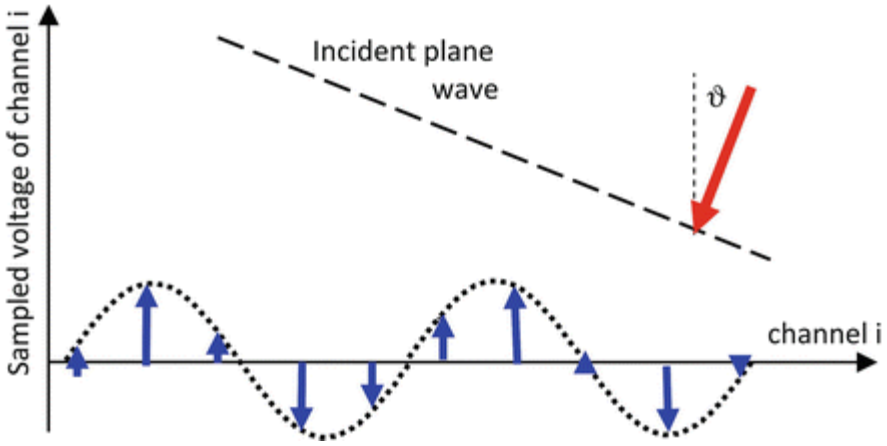

Fig. 14
Real part of IF samples for a slanted incidence of a wave

The beamwidth of the subarray(s) in such an approach must be sufficient to cover the angle range of interest for the respective application. At least two of the subarrays should be placed at a distance as close as possible to half a wavelength to ensure an unambiguous cross-range resolution, but further subarrays may be arranged at larger but different distances between each other, so a high lateral resolution can be achieved, while the different distances can be optimized to remove ambiguities (grating lobes) (Moffet 1968; Md Tan et al. 2008; Feger et al. 2009). Combining this beamforming with configurations as described in the following, even an effective aperture width larger than the physical one can be achieved.

MIMO Concepts for Automotive Radar

In Kees et al. (1995), a concept was proposed to improve the angular resolution of an imaging radar system by transmitter location multiplexing. Today, this concept partly is called MIMO radar (multiple in, multiple out), although in most cases transmitters or receivers (Mayer et al. 2006) are operated successively. Just recently, a concept has been presented to simultaneously transmit via several channels in frequency domain multiplex and to receive in parallel by a respective number of receivers (Pfeffer et al. 2013).
According to antenna theory, the angular distribution of the radiated fields (radiation diagram) of an antenna is proportional to the Fourier transform of its aperture distribution in the respective plane. On the other hand, the signal transmitted from one antenna and received by another one is proportional to the multiplication of the radiation diagrams of these two. Consequently, this product can also be derived from an aperture distribution formed by the convolution of the two individual aperture distributions. Superposition of the measurements from n transmits and m receive subarrays then results in the convolution of the respective excitation distributions (Fig. 15). Accordingly, the configuration as given in the example in Fig. 15 results in a synthetic antenna array with densely arranged subarrays. Other combinations of transmit and receive antennas even result in an increased aperture (Mayer et al. 2006). Weighting the individual measurements

with complex numbers (representing phase and amplitude adjustments), different beam directions or modifications of the radiation diagram can be adjusted and evaluated simultaneously.

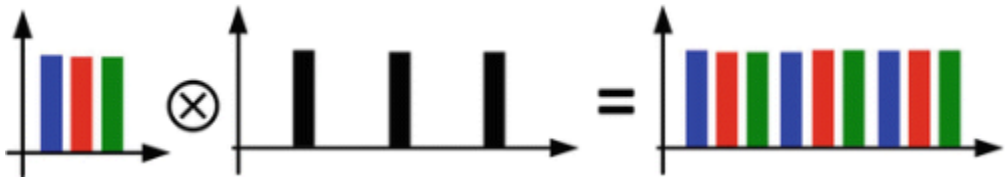

Fig. 15
Convolution principle for MIMO radar

Fabrication, Packaging, and Mounting Considerations

As already mentioned in the introduction, automotive radars have to operate in a temperature range from −40 °C up to 85 °C or even higher, they have to withstand shock and vibrations, and they have to operate under conditions of rain, snow, or ice. Materials, fabrication processes, packaging as well as mounting of the sensor therefore have to be selected carefully.

Substrate materials need to be suitable for the mm-wave frequency, their physical and electrical properties should be reasonably constant over the temperature range, and they should not absorb moisture. On the other hand, standard microwave substrates may be rather expensive, so a compromise has to be made in this respect. Etching of the planar structures should, as far as possible, be done using standard printed circuit board (PCB) processes but may require accuracies down to 20 µm for the 77 GHz frequency range - this also poses a great challenge toward tolerance-optimized antenna design. Metal surfaces, in addition, need to be protected against corrosion by suitable plating.

Antennas need to be connected to the millimeter-wave circuits and/or MMICs. While bonding at 24 GHz is still not too critical, this provides major efforts and therefore higher cost at 77 GHz. Typically, MMICs have to be placed in some cavity in the circuit board, and bonding is done in the same level to keep parasitics as low as possible (see also the first application example in this chapter). One way out of this is to provide a suitable package for the MMIC as described in Fig. 16 (Wojnowski et al. (2011)), known as eWLB packaging. The MMIC is embedded into a plastic mold, further metallization levels connect the MMIC to lines on the mold, and a ball grid array then allows an easy interconnect to the circuit board, possibly directly to the antenna substrate. In this way, the assembling of antenna and MMICs is feasible without specialized and costly equipment.

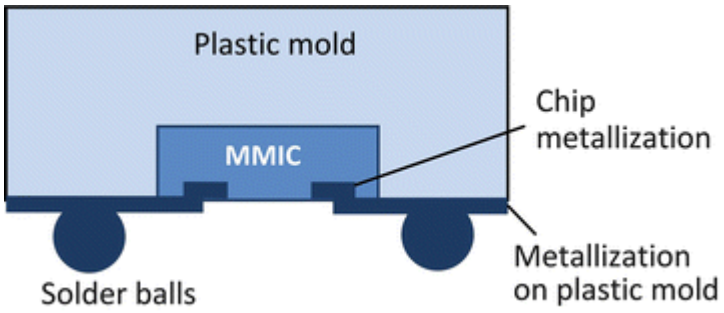

Fig. 16
eWLB package

The antenna and the radar sensor as a whole, finally, have to be protected by a suitable package. This typically is done by an overall housing, as can be seen also at the examples given in the following section. The cover in front of the antenna (radome) must be transparent to the electromagnetic wave in the respective frequency range, leading to an optimized thickness for the used plastic materials in the order of multiples of half a guide wavelength within the material. This optimized thickness only is perfect for one angle of radiation. For all other angles, there is performance degradation due to reflection. Major efforts are necessary to keep the influence of such a reflection below a given threshold. If the cover is close to the antenna, even a codesign of antenna and cover has to be done.

Mounting of the radar sensor at the car requires a position from which the radar can cover the relevant angle of view, but space limitations and overall car design concepts require some compromise; so typical mounting positions are behind the radiator grille and the bumper. Today, the bumper often is painted, and efforts have to be done to ensure a sufficient

transparency of the bumper, even with paintings containing metallic particles. This can be done by optimizing the thickness of the bumper material or by adding some matching layer in front of the radar (Fitzek et al. 2010).
Furthermore, during operation, the radome must not be covered by layers of water, ice, or snow; this would severely deteriorate its performance. To avoid this, a protected mounting position, e.g., behind the bumper, a water-repellent radome surface, or a suitable form or orientation of the radome to blow away water or snow just by the natural airstream of the car, can be selected.

Application Examples for Automotive Antennas

Bosch Sensor LRR3

The LRR3 automotive radar sensor of Bosch came onto the market in 2009. It is based on the FMCW principle, and the mm-wave transmit and receive circuits are integrated on a four-channel SiGe monolithic chip (Winkler et al. 2008) connected to four single microstrip patch antennas combined with parasitic elements to adjust the bandwidth and beamwidth. In the original version, the MMIC is mounted into a cavity in the printed circuit board and bonded to the antenna feed lines. In an advanced version, eWLB packaging as described above is used for the MMIC. The antenna elements are tilted by 45° to reduce interference from oncoming cars. The antenna elements serve as feeds for a lens antenna (Binzer et al. 2007), resulting in four narrow beams. An exploded view of the complete sensor and the planar antenna section is shown in Fig. 17. With overlapping radiation diagrams of the beams (Fig. 18), the angular detection of targets is done by monopulse principles between two neighboring beams, resulting in a resolution considerably better than the beamwidth, provided that only one target is in the respective range cell.

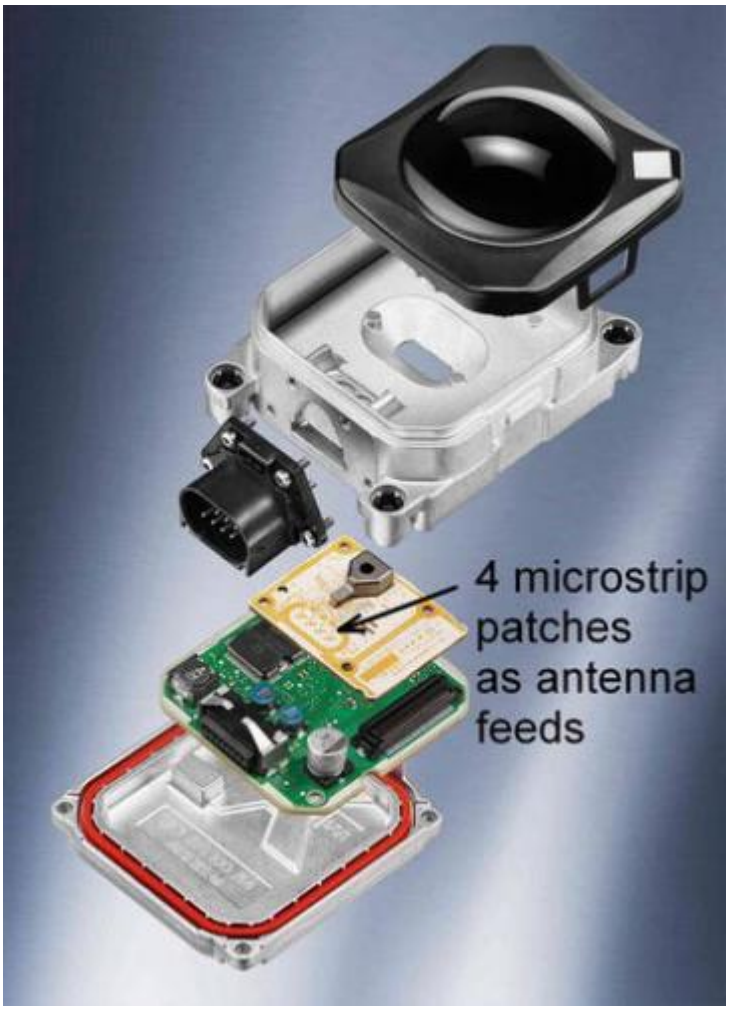

Fig. 17
Exploded view on the Bosch LRR3 sensor and details of the planar antenna elements feeding the lens (Sensor photograph provided by Bosch)

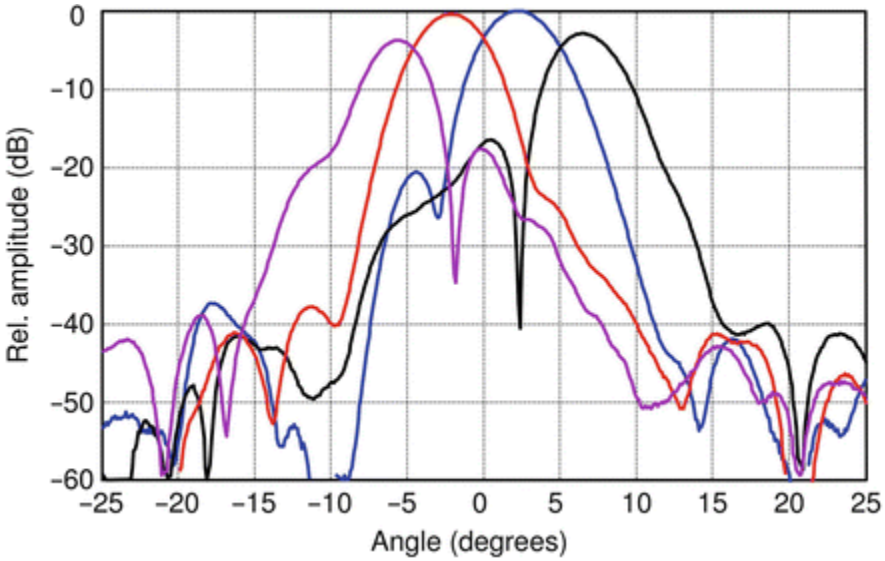

Fig. 18
Azimuth radiation diagrams of the four beams of the LRR3 radar (Fig. 16)

Continental Sensor ARS300

Also in 2009, Continental ADC introduced its third generation of automotive radar with completely new features and a novel approach for the radar antenna. The antenna of the ARS300 scans with a narrow beam over a given azimuth range; it performs auto alignment and is of compact size.

As can be seen in Fig. 19, the entire arrangement consists of a dielectric waveguide in the vicinity of a grooved rotating drum and a folded space consisting of a polarizing grid, also serving as mechanical protection and radome, and a focusing reflectarray. A photograph of the opened sensor is given in Fig. 20. The basic radiation structure is a dielectric guide with propagation constant k_d. The drum is placed close to the dielectric waveguide, and the metal ridges between the grooves of the drum form periodic perturbations at which the dielectric guide radiates (Fig. 19); the radiated partial fields superpose to form the overall far field radiation. For a given direction of radiation, these partial fields must superimpose in phase. According to Fig. 21, the following relation must hold

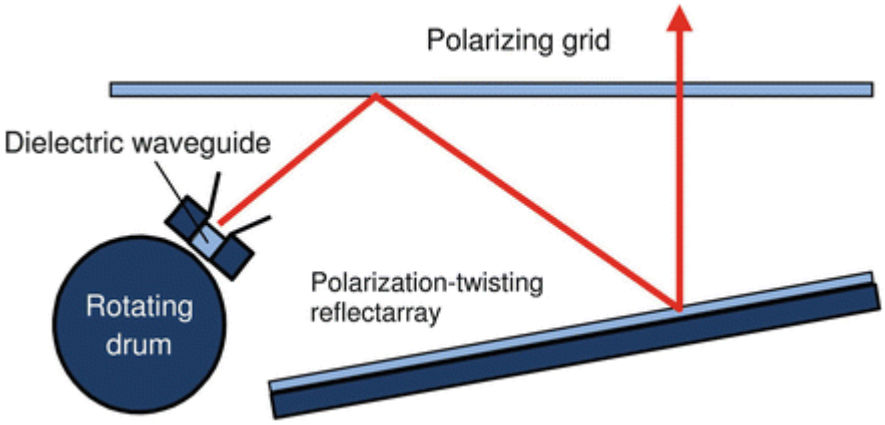

Fig. 19
Principal cross section of the Continental ARS 300 antenna

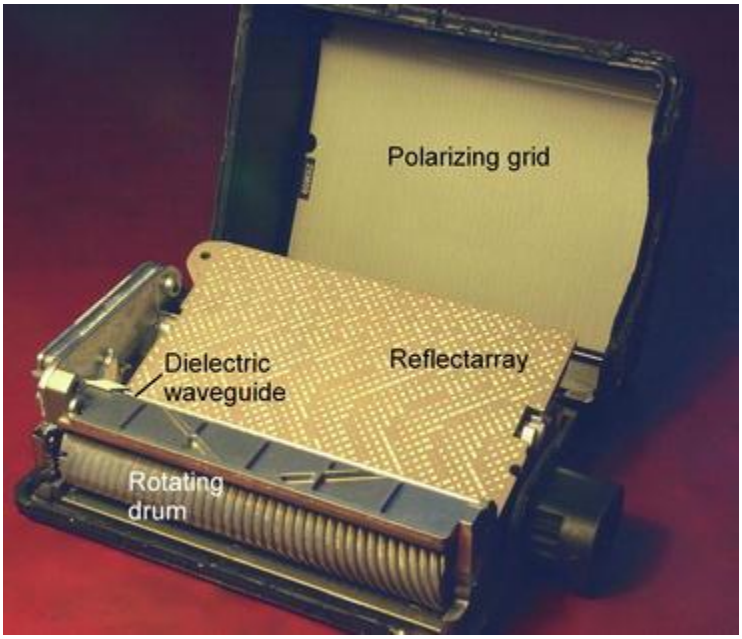

Fig. 20
Photograph of the Continental ARS 300 sensor with opened cover (own photograph)

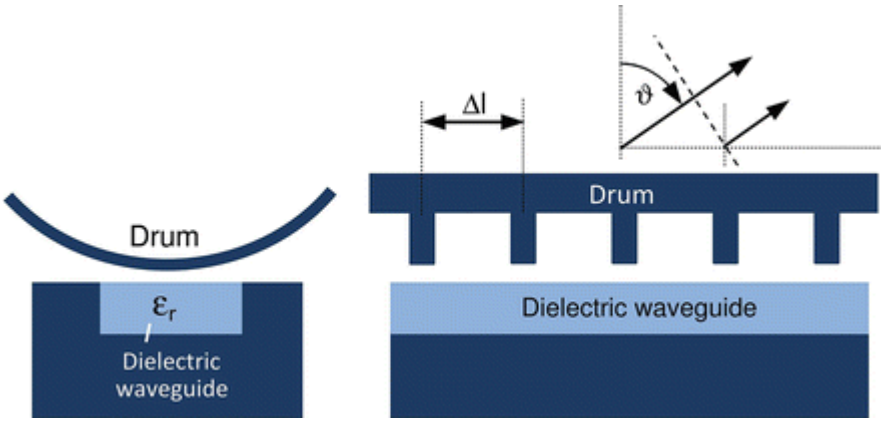

Fig. 21
Details of radiating dielectric guide

$$k_0 \Delta l \ \sin(\delta) + 2\pi = k_d \Delta l \tag{3}$$

where k_0 and k_d are the phase constants of free space and the dielectric guide, respectively, and Δl is the distance between the metal ridges (Fig. 21).

To scan the radiated beam over a given angle, the period of the grooves has to be modified - the groove period depends on the rotational angle, and the actual groove period in the direct vicinity of the guide determines the direction of the radiated beam. Rotating the drum then leads to a scanning of the beam (Manasson et al. 1996). A great effort has been spent in designing the drum in a way to find the optimum shape and size of the grooves such that at each azimuth angle a beam of a given scan angle with sidelobes below a prescribed threshold is obtained. A unique feature of this waveguide drum unit is that it contains different angular sections in which both the direction of radiation and the beamwidth can be altered such that different sensor modes from short to long range (up to 200 m) can be covered by a single setup.

Additionally, the radiated wave has to be formed to provide a narrow diagram in elevation as well. This is done by a folded reflectarray configuration as described earlier (see also Fig. 7). The required polarizer is integrated into the cover of the sensor such that the beam radiated from the dielectric waveguide/drum unit is reflected toward a reflectarray consisting of a dielectric layer glued onto a conducting plate. Phase angles are adjusted such that a narrow beam results in elevation, together with the necessary polarization twisting. Both the polarizing grid printed to the sensor cover and the reflectarray can clearly be seen in Fig. 19. Measurements of the radiation diagrams have been done using the complete radar, resulting in two-way diagrams. A selection of far field radiation diagrams for different drum positions can be seen in Fig. 22. Two-way beamwidths are in the range of 2.5°.

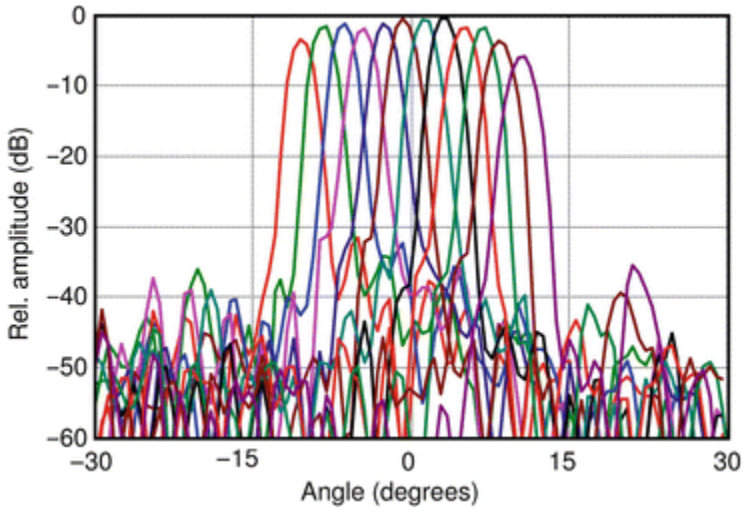

Fig. 22
Selected two-way azimuth radiation diagrams of the Continental ARS 300 sensor

In addition, this antenna exhibits another unique feature. While the headlights of a car can be adjusted in elevation by any skilled person, this is different for a radar sensor with its non-visible radiation. With this antenna, the reflectarray can be tilted to some extent by a motor unit which performs an auto alignment in elevation.

Experimental 79 GHz LTCC-Based Sensor with Grid Antennas

For high-density 3D integration, low- and high-temperature cofired ceramics (LTCC, HTCC) are gaining increasing interest. The starting point for their fabrication is mixtures of ceramic and glass powder together with binding agent for LTCC and solely ceramic powder with binding agent for HTCC. These materials are pressed into thin sheets (one tenth or a few tenth of a millimeter thick) and cut into suitable panels. In the first step, holes for vias are punched into the sheets and filled with metal paste. Following this, screen printing is applied to print metal patterns onto each sheet. Finally, a required number of sheets (even several tens of sheets) are laminated and pressed together, precut, and fired. For LTCC, only the glass powder needs to melt, so temperatures in the range of 900 °C are sufficient. For HTCC, the ceramic powder must be joined together, so temperatures of 1,600 °C are required. For very fine and accurate structures on the outer sides of the multilayer, even sputtered and electroplated metal with standard etching processes can be added (partly called "fine line" techniques (Brunner et al. 2012)). Including these processes, LTCC can be extended to the design of highly integrated millimeter-wave circuits.

This technique was applied to develop an experimental 79 GHz short-range sensor using grid antennas and a four-channel SiGe radar front end (Bauer et al. 2013). A principal cross section of the multilayer circuit is given in Fig. 23. The multilayer contains 12 layers of 0.118 mm thickness each. The dielectric constant for the material used here is 7.4. Vias can be fabricated down to a diameter of 0.1 mm, easily enabling SIW structures; the effective SIW width is about 1.2 mm. Two grid antennas with opposite orientations are located on the top surface, fed by probes to a first layer of SIW. An E-plane T-junction feeds the signals to a lower level SIW; from there, another probe-type transition provides a connection to a planar symmetric line at the backside where the MMIC is located and bonded to the planar lines.

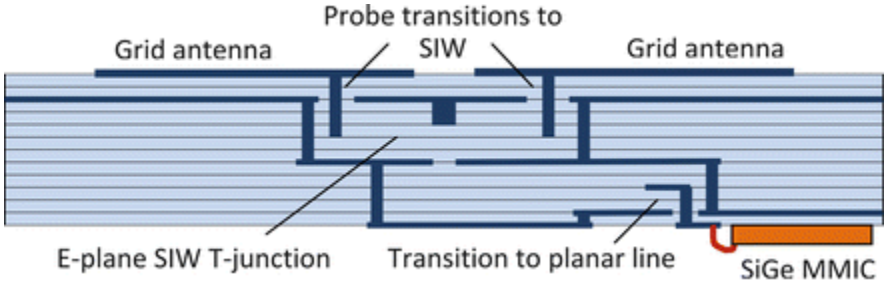

Fig. 23
Cross section of LTCC sensor

A photograph of the antenna side of the sensor together with a section of the backside with the MMIC is depicted in Fig. 24. While the LTCC substrate has dimensions of 23 × 23 mm, the overall usable size for the antenna arrangement is 13 × 20 mm. This consists of four chains of grid antennas, each connected to one channel of the MMIC. As at least two channels need to be closely spaced to ensure unambiguity, two chains consist of single rows, while the other two are double chains to increase the overall (processed) signal output (at the cost of a reduced angle of view) and placed at larger distances to the single chains. Mid-to-mid distances between the antenna rows are 3.6, 2.2, and 5.4 mm. Radiation diagrams of a single-row antenna are plotted in Fig. 25; beamwidths in elevation and azimuth are about 15° and 60°, respectively. The elevation diagram of the double-chain antenna is equal to that of the single-row one; the azimuth diagram of the double-row antenna has a 3 dB beamwidth of 40°.

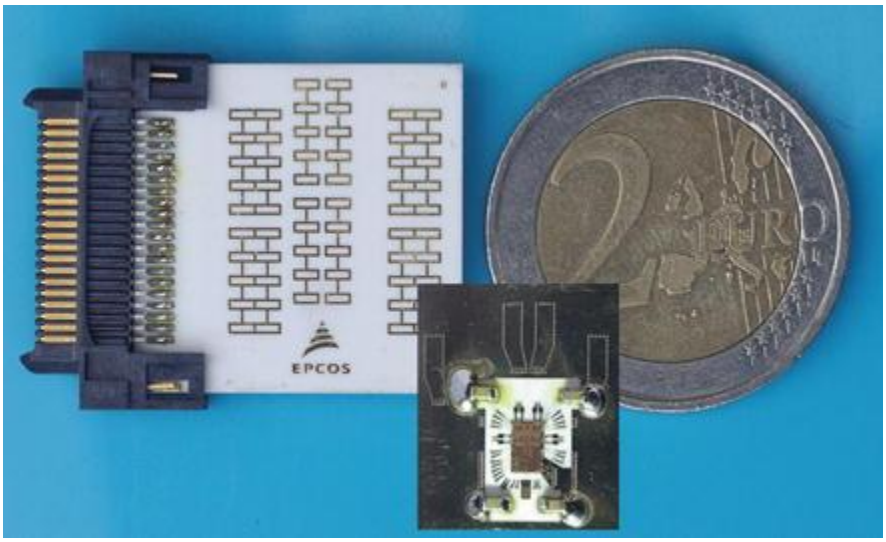

Fig. 24
Photograph of the 79 GHz LTCC sensor; antenna side and MMIC side in inset (own photograph)

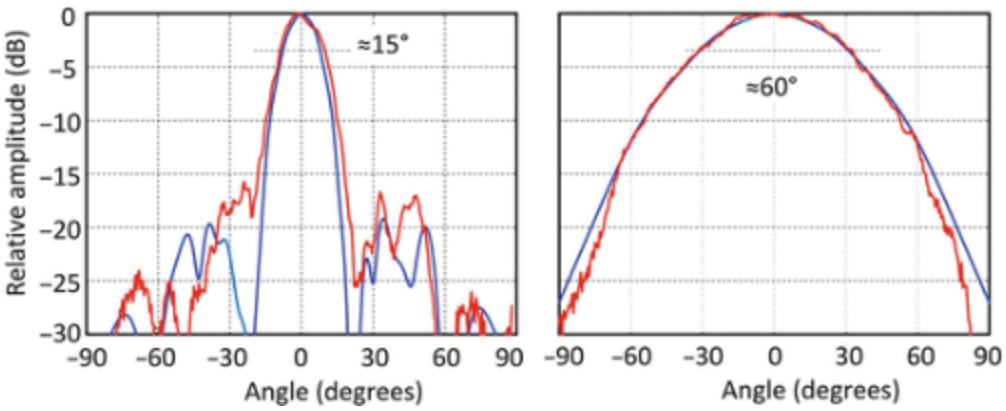

Fig. 25
Elevation (E-plane) and azimuth (H-plane) radiation diagrams of a single-row grid antenna. Blue simulation, red experiment

Each radar channel is able to both transmit (FMCW) and receive; all channels are active in receiving whatever channel is transmitting. MIMO principles with optimized weighting functions are then applied for cross-range imaging according to Feger et al. (2009). According to the convolution principle, ten different synthetic antenna positions result with a nearly doubled antenna aperture. The response to a target then has a 3 dB width of about 10° at the broadside (Bauer et al. 2013). Together with the FMCW principle for range, a typical radar image for two targets is shown in Fig. 26. With this experimental sensor, a range of up to 20 m can be covered; employing a new LTCC material with lower losses and a further optimization of the backside transition to the MMIC will increase range further. Of course, also a larger antenna size will do the same.

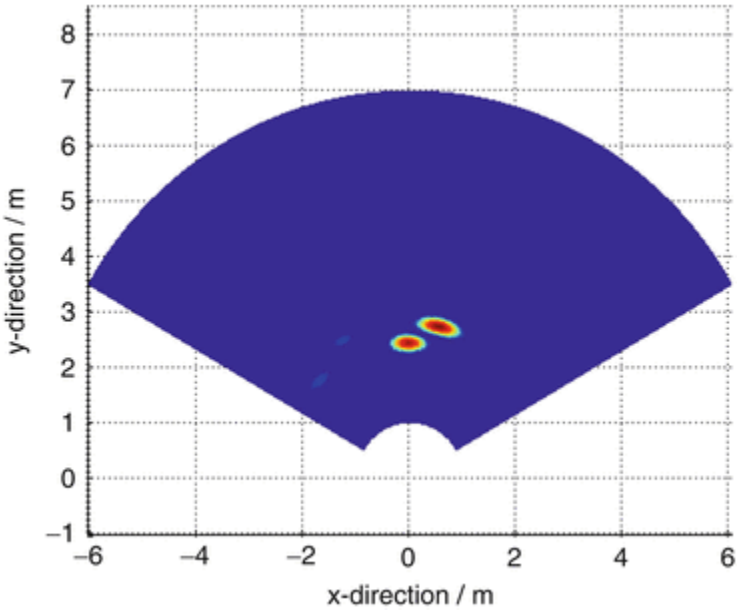

Fig. 26
Close-range image of two targets

Conclusion

After an introduction to automotive radar sensors and their principle architecture, this chapter provides a guide to different types of antennas for automotive radars. While in the early approaches more or less standard antenna configurations were dominating, different types of planar antennas and array antennas have been employed later on. As shown in the second system example, also different antenna types like a dielectric line-based radiator with a mechanical scanning unit and a printed and folded reflectarray antenna are combined for best performance. Presently, the original function of "stand-alone" antennas is being replaced by an overall arrangement of antenna elements and arrays, transmit/receive configuration, and digital signal processing, as it is demonstrated by digital beamforming together with (quasi-) MIMO concepts. The latter allows a reduction of transmit/receive modules and antenna elements, and it even allows to generate synthetic apertures larger than the physical ones.

Signal processing is also a means to further increase resolution in all radar relevant domains, i.e., range, cross range, and Doppler frequency. In the present commercial sensors, real-time signal processing is still limited to the basic functions, but soon high-resolution methods like MUSIC (Schmidt 1986), ESPRIT (Roy et al. 1986), or autoregressive (AR) signal estimation (Proakis and Manolakis 1996) will be considered. In a number of studies, AR signal estimation has proven to be quite robust in automotive applications, e.g., Mayer et al. (2006). In cross range - where the antenna configuration is relevant - beamforming leads to a number of sampled values from which the lateral target distribution is calculated using an FFT. Explained in a very simple way, such a series of sampled values can be modeled by a kind of digital filter, and with this, new artificial sampling values can be generated on either side of the original series, typically increasing the number of samples by 2 or 3. An FFT over the enlarged series then results in an improved cross-range resolution, equivalent to an antenna aperture of twice or three times as wide.

With more stringent requirements for safety application, also an improved resolution with respect to elevation gets more and more important - is there any target which the vehicle can run over or pass below, or is it a relevant obstacle? As a consequence, systems - and therefore the antenna configurations - need to be extended, either to switch or scan in elevation as well, or an extra antenna element may be added to observe higher elevation angles.

As discussed in the second chapter, operation frequency of automotive sensors mostly is shifting from the 24 GHz frequency range to the 76/77 and 77/81 GHz range; the driving motivation is toward smaller sensors; basically, the effective size is determined by the antenna. Based on this, also higher frequency ranges are under first investigations (Köhler et al. 2013). Frequencies may be in the 120 or 150 GHz range. For the same antenna aperture as with lower frequencies, gain is increased, or for the same gain, antenna dimensions get smaller. One has to be aware, however, that

with smaller antenna aperture size, the received power decreases as well. From the antenna design point of view, a simple scaling of the structure seems to be possible; care has to be taken for increased losses and more critical tolerance requirements. Semiconductor devices show increasing cutoff frequencies (Pfeiffer 2012), but output power will be lower and receiver noise figure higher. Nevertheless, estimations in Köhler et al. (2013) show that MRR and SRR sensors should be feasible. Another challenge with higher frequencies will be interconnects, but efforts are going on to integrate antenna elements directly on a MMIC or providing specific packaging technologies with potentially integrated antenna elements provided by the MMIC manufacturer, e.g., Wojnowski et al. (2011) and Hasch et al. (2012).

Cross-References

- Beam-Scanning Leaky-Wave Antennas
- Grid Antenna Arrays
- Microstrip Patch Antennas
- Millimeter-Wave Antennas and Arrays
- Reflectarray Antennas
- Substrate Integrated Waveguide Antennas
- Waveguide Slot Antennas and Arrays

Acknowledgments Thanks are due to Bosch and Continental ADC for providing part of the material for this chapter. Other parts of the results shown here have been achieved by projects funded via the "RoCC project (project number 13 N9824) of the German Federal Ministry of Education and Research (BMBF)" and the "Austrian BMVIT and the Austrian Research Promotion Agency (FFG) within the co-funded project InRaS in the strategic objective FIT-IT Systems on Chip."

References

- Asano Y, Ohshima S, Harada T, Ogawa M, Nishikawa K (2001) Proposal of millimeter-wave holographic radar with antenna switching. IEEE Inter Microw Symp 2:1111-1114
- Bauer F, Menzel W (2011) A 79 GHz microstrip grid array antenna using a laminated waveguide feed in LTCC. In: IEEE AP-S/URSI symposium 2011, Spokane, pp 2067-2070
- Bauer F, Wang X, Menzel W, Stelzer A (2013) A 79-GHz radar sensor in LTCC technology using grid array antennas. IEEE Trans Microw Theory Tech 61:2514-2521
- Bauer F, Menzel W (2013a) A 79-GHz resonant laminated waveguide slotted array antenna using novel shaped slots in LTCC. IEEE Antennas Wirel Propag Lett 12:296-299
- Bauer F, Menzel W (2013b) A 79-GHz planar antenna array using ceramic filled cavity resonators in LTCC. IEEE Antennas Wirel Propag Lett 12:910-913
- Binzer T, Klar M, Groß V (2007) Development of 77 GHz radar lens antennas for automotive applications based on given requirements. In: 2nd international ITG conference on antennas (INICA '07 Munich), pp 205-209
- Brunner S, Stadler M, Wang X, Bauer F, Aichholzer K (2012) Advanced high frequency LTCC technology for applications beyond 60 GHz. In: Proceedings of the 8th international conference on Ceramic Interconnect and Ceramic Microsystems Technologies, Erfurt, pp 77-81
- Camiade M, Domnesque D, Ouarch Z, Sion A (2000) Fully MMIC-based front end for FMCW automotive radar at 77 GHz. In: Proceedings of the 30th European Microwave conference Paris, pp 1-4
- Carver KR, Mink JW (1981) Microstrip antenna technology. IEEE Trans Antennas Propag 9:2-24
- Conti R, Toth J, Dowling T, Weiss J (1981) The wire grid microstrip antenna. IEEE Trans Antennas Propag 29:157-166
- Feger R, Wagner C, Schuster S, Scheiblhofer S, Jäger H, Stelzer A (2009) A 77-GHz FMCW MIMO radar based on a SiGe single-chip transceiver. IEEE Trans Microw Theory Tech 57:1020-1035
- Fitzek F, Rasshofer RH, Biebl EM (2010) Metamaterial matching of high-permittivity coatings for 79 GHz radar sensors. In: European Microwave conference, Paris, pp 1401-1404
- Frei M, Bauer M, Menzel W, Stelzer M (2011) A 79 GHz differentially fed grid array antenna. In: European Microwave conference, Manchester, pp 1320-1323
- Gresham I, Jain N, Budka T, Alexanian A, Kinayman N, Ziegner B, Brown S, Staecker P (2001) A compact

manufacturable 76-77-GHz radar module for commercial ACC applications. IEEE Trans Microw Theory Tech 49:44-58

- Gresham I, Jenkins A, Egri R, Eswarappa C, Kinayman N, Jain N, Anderson R, Kolak F, Wohlert R, Bennett J, Lanteri J-P (2004) Ultra-wideband radar sensors for short-range vehicular applications. IEEE Trans Microw Theory Tech 52:2105-2120
- Hasch J, Topak E, Schnabel R, Zwick T, Weigel R, Waldschmidt C (2012) Millimeter-wave technology for automotive radar sensors in the 77 GHz frequency band. IEEE Trans Microw Theory Tech 60:845-860
- Hirokawa J, Ando M (2000) 76 GHz post-wall waveguide fed parallel plate slot arrays for car-radar applications. IEEE Int Symp Antennas Propag 1:98-101
- Hymans AJ, Lait J (1960) Analysis of a frequency-modulated continuous-wave ranging system. Proc IEE Part B Electron Commun Eng 107:365-372
- James JR, Hall PS, Wood C (1981) Microstrip antenna theory and design. Peregrinus, London
- Kees N, Schmidhammer E, Detlefsen J (1995) Improvement of angular resolution of a millimeterwave imaging system by transmitter location multiplexing. IEEE Int Microw Symp 2:969-972
- Köhler M, Hasch J, Blöcher HL, Schmidt L-P (2013) Feasibility of automotive radar at frequencies beyond 100 GHz. Int J Microw Wirel Technol 5:49-54
- Kraus J (1964) A backward angle-fire array antenna. IEEE Trans Antennas Propag 12:48-50
- Massen J, Frei M, Menzel W, Möller U (2013) A 79 GHz SiGe short-range radar sensor for automotive applications. Int J Microw Wirel Technol 5:5-14
- Mayer W, Gronau A, Menzel W, Leier H (2006) A compact 24 GHz sensor for beam-forming and imaging. In: 9th international conference on control, automation, robotics and vision (ICARV 2006 Singapore), pp 153-158
- Md Tan MN, Rahim SKA, Ali MT, Rahman TA (2008) Smart antenna: weight calculation and side-lobe reduction by unequal spacing technique. In: IEEE international RF and microwave conference, Kuala Lumpur, pp 441-445
- Manasson V, Sadovnik L, Mino R (1996) MMW scanning antenna. IEEE Aerosp Electron Syst Mag 11:29-33
- Meinel HH, Dickmann J (2013) Automotive radar: from its origin to future directions. Microw J 56:24-40
- Menzel W, Pilz D, Al-Tikriti M (2002) MM-wave folded reflector antennas with high gain, low loss, and low profile. IEEE Antennas Propag Mag 44:24-29
- Millitech Corporation (1994) Crash avoidance FLR sensors. Microw J 37:122-126
- Moffet A (1968) Minimum-redundancy linear arrays. IEEE Trans Antennas Propag 16:172-175
- Pfeffer C, Feger R, Wagner C, Stelzer A (2013) FMCW MIMO radar system for frequency-division multiple TX-beamforming. IEEE Trans Microw Theory Tech 61:4262-4274
- Pfeiffer UR (2012) Silicon CMOS/SiGe transceiver circuits for THz applications. In: IEEE 12th topical meeting on silicon monolithic integrated circuits in RF systems (SiRF), Santa Clara, pp 159-162
- Proakis JG, Manolakis DG (1996) Digital signal processing: principles, algorithms, and applications. Prentice-Hall International, Upper Saddle River
- Roy R, Paulraj A, Kailath T (1986) ESPRIT - a subspace rotation approach to estimation of parameters of cisoids in noise. IEEE Trans Acoust Speech Signal Process 34:1340-1342
- Russell ME, Crain A, Curran A, Campbell RA, Drubin CA, Miccioli WF (1997) Millimeter-wave radar sensor for automotive intelligent cruise control (ICC). IEEE Trans Microw Theory Tech 45:2444-2453
- Sakakibara K, Mizutani A, Kikuma N, Hirayama K (2006) Design of narrow-wall slotted hollow waveguide array for arbitrarily linear polarization in the millimeter-wave band. In: IEEE international symposium on antennas propagation, Albuquerque, 3141-3144
- Schmidt R (1986) Multiple emitter location and signal parameter estimation. IEEE Trans Antennas Propag 34:276-280
- Shino N, Uchimura H, Miyazato K (2005) 77 GHz band antenna array substrate for short range car radar. In: IEEE MTT-S international microwave symposium Long Beach, pp 2095 - 2098
- Stelzer A, Feger R, Jahn M (2010) Highly-integrated multi-channel radar sensors in SiGe technology for automotive frequencies and beyond. In: ICECom conference, Dubrovnik, pp 1-11
- The (new) Cadillac Database©Dream Cars on Cadillac Chassis (2013) http://www.cadillacdatabase.org/Dbas_txt/Drm_cycl.htm. Last updated 23 May 2013
- Tokoro S, Kuroda K, Kawakubo A, Fujita K, Fujinami H (2003) Electronically scanned millimeter-wave radar for pre-crash safety and adaptive cruise control system. In: Proceedings of the IEEE intelligent vehicles symposium

Columbus, pp 304-309
- Winkler V, Feger R, Maurer L (2008) 79 GHz automotive short range radar sensor based on single-chip SiGe-transceivers. In: European Microwave conference, Amsterdam, pp 1616-1619
- Wojnowski M, Lachner R, Böck J, Wagner C, Starzer F, Sommer G, Pressel K, Weigel R (2011) Embedded wafer level ball grid array (eWLB) technology for millimeter-wave applications. In: IEEE 13th electronics packaging technology conference (EPTC), Singapore, pp 423-429
- Woll JD (1995) VORAD collision warning radar. In: IEEE international radar conference, Alexandria, pp 369-372
- Xu JF, Hong W, Chen P, Ke W (2009) Design and implementation of low sidelobe substrate integrated waveguide longitudinal slot array antennas. IET Microw Antennas Propag 4:790-797
- Zhang B, Zhang YP (2012) Grid array antennas with subarrays and multiple feeds for 60-GHz radios. IEEE Trans Antennas Propag 60:2270-2275

Antennas in Automobile Radar

Wolfgang Menzel	Institute of Microwave Techniques, University of Ulm, Ulm, Germany
DOI:	10.1007/SpringerReference_384212
URL:	http://www.springerreference.com/index/chapterdbid/384212
Part of:	Handbook of Antenna Technologies
Editor:	PhDs Zhi Ning Chen
PDF created on:	January, 02, 2015 04:11